*IFSCC 2025 full paper (IFSCC2025-299)*

# Revitalizing the potential of the skin microbiome for UV defense

**Nakako Shibagaki[1*], Mamiko Yano[1], Ami Kaneshima[1], Rie Kamezono[1], and Hiroko Manabe[1]**

[1] Mirai Institute, Shiseido Co., Ltd.
*Nakako Shibagaki, 1-2-11 Takashima, Nishi-ku, Yokohama, Kanagawa 220-0011, Japan
nakako.shibagaki@shiseido.com

## 1. Introduction

Ultraviolet radiation (UVR) is a pervasive environmental factor known to significantly affect skin health. While its role in inducing oxidative stress and contributing to premature skin aging is well documented (1), the impact of UVR on the skin microbiome remains an emerging area of research. The skin microbiome, a complex community of microorganisms residing in the skin, plays a vital role in maintaining skin homeostasis and protecting against external aggressors, including UVR. This symbiotic relationship between the skin and its microbiome is crucial for preserving the skin's barrier function and immune responses. Understanding how UVR influences the composition and function of the skin microbiome is essential for developing strategies to mitigate its adverse effects. There are previous studies that report artificial one-shot exposure to medical UVR modifies the skin microbiome when checked 24 hours after exposure (2,3). We aimed to more deeply explore how the skin microbiome evolves under the effect of UVR exposure in daily life, since it evolves to reach a certain balance during the season of high UV when various factors affect the skin microbiome both positively and negatively (i.e., high UVR likely suppresses growth of the skin microbiome and immune system (4), and high temperatures cause increased sebum and sweat secretion in skin, which is favorable for skin microbiome propagation). Furthermore, we aimed to develop a postbiotic ingredient to compensate for the functions diminished in the UVR-altered skin microbiome in order to mitigate UVR-related skin damage.

## 2. Materials and methods

### Human study design

Healthy Japanese women were recruited for the study. One group consisted of participants who regularly use suncare products with SPF 50+ on their faces, while the other group was comprised of individuals who rarely use sunscreen with SPF 50+. The participants in both groups were in the same age range: 47.8 ± 4.4 years (n = 22) and 47.4 ± 5.1 years (n = 22), respectively. Standard exclusion criteria were applied during recruitment. The participants were instructed to continue using their regular skincare products, to refrain from receiving any beauty esthetic treatments starting one month prior to the study, and to avoid activities involving excessive sun exposure for at least two weeks before. They were also asked to avoid stressful activities during the week leading up to the test. The study was approved by the Human Test Ethics Council of Shiseido Co., Ltd. under the approval number C10177.

The participants visited the test site in March and September 2022. Upon arrival, they were asked to cleanse their faces with bar soap and gently pat their skin dry with sterilized gauze. After resting in a climate-controlled room set at 23 °C and 45 % humidity for 20 minutes, stratum corneum samples were collected from their foreheads for the microbiome analysis and instrumental measurements conducted.

**Sampling for microbiome analysis**

UV-treated Corneofix™ tape (Courage+Khazaka electronic GmbH, Koln, Germany) was applied to the forehead of each participant. Two strips of tape were used consecutively at the same site, and only the second strip of tape was used for subsequent analysis. After removal from the skin, the protein concentration was measured using a SquameScan 850 (Heiland electronic GmbH, Wetzlar, Germany), and the result was used to normalize the total number of bacterium collected and then stored in a DNA/RNA Shield™ (Zymo Research, Irvine, CA, USA).

**16S analysis**

**DNA extraction**: DNA was extracted using a ZymoBIOMICS®-96 MagBead DNA Kit (Zymo Research).
**Targeted library preparation:** The DNA samples were prepared for targeted sequencing with a Quick-16S™ NGS Library Prep Kit (Zymo Research). Primers were custom designed by Zymo Research to provide the best coverage of the 16S gene while maintaining high sensitivity. The primer set used in this project was the Quick-16S™ Primer Set V1–V2 (Zymo Research).
**Sequencing:** The final library was sequenced on an Illumina® MiSeq™ with a v3 reagent kit (600 cycles). The sequencing was performed with a 10 % PhiX spike-in.
**Bioinformatics analysis**: Unique amplicon sequences were inferred from raw reads using the DADA2 pipeline (5). Chimeric sequences were removed as part of this process. Taxonomy classification was performed using UCLUST from QIIME v.1.9.1. with reference to the Zymo Research Database, an internally designed and curated 16S database. Composition visualization, alpha-diversity, and beta-diversity analyses were also performed with QIIME v.1.9.1 (6).
**Absolute abundance quantification:** A quantitative real-time PCR was set up with a standard curve made with plasmid DNA containing one copy of the 16S gene prepared in 10-fold serial dilutions. The primers used were the same as those used in the targeted library preparation phase. The resulting equation was used to calculate the number of gene copies in the reaction for each sample. The PCR input volume (2 µl) was used to calculate the number of gene copies per microliter in each DNA sample. The number of genome copies per microliter DNA sample was calculated by dividing the gene copy number by an assumed number of gene copies per genome. The value used for 16S copies per genome was 4. The amount of DNA per microliter was calculated based on an assumed genome size of $4.64 \times 10^6$ bp (*Escherichia coli*) or $1.20 \times 10^7$ bp. All statistical analyses were conducted using paired t-tests.
**Instrumental measurement:** Sebum levels on the surface of the facial skin were measured using a Sebumeter (SM815; Courage and Khazaka electronic GmbH). Skin color parameters, such as the melanin index, a*, b* and L*, were measured using a CM-700d Spectrophotometer (Konica Minolta, Tokyo, Japan).

**Bacterial culture**

Bacterial strains isolated from clinical samples of stratum corneum were precultured in the Soybean Casein Digest medium. After washing them in saline buffer twice, bacterial cells were used for 4-VG production assay, in which the cells were grown in media containing 1 x M9

salts (Merck KGaA, Darmstadt, Germany), 2 mM $MgSO_4$, 0.1 mM $CaCl_2$, 0.1 % yeast extract, 0.2 % glucose, and 0.01 % ferulic acid at 37 ℃ with 140 rpm.

**4-vinylguaiacol production measurement**

For LC analysis, the bacterial culture was harvested at the designated time points, mixed with an equal volume of acetonitrile, and stored at −20 ℃ until analysis. After sonication and centrifugation to remove insoluble cell debris, a supernatant was used for LC analysis. LC separation was performed at 40 ℃ using a CAPCELL PAK C18 AQ column (150 mm x 2.0 mm I.D., 3 µm particle size). The isocratic mobile phases consisted of a 50:50 (v/v) mixture of 0.1 % $H_3PO_4$ in water and 0.1 % $H_3PO_4$ in MeOH, delivered at a flow rate of 200 µL per minute. The injection volume was 20 µL, and peak areas were measured at 280 nm.

**Sanger sequencing of the 16S rRNA gene**

A Bacterial 16S rDNA PCR Kit (Takara Bio Inc., Shiga, Japan) was used for amplification. Amplified fragments were purified by using a QIAquick PCR Purification Kit (Qiagen, Hilden, Germany) and subjected to Sanger sequencing.

**Gene expression in keratinocytes**

Normal Human Epidermal Keratinocytes (NHEK) from a newborn foreskin was obtained from Kurabo (Osaka, Japan). Cells were grown in HuMedia-KG2 (Kurabo) in an incubator with a humidified atmosphere of 5% $CO_2$ at 37°C and inoculated in 6 well plates at 50,000 cells/mL. After culturing for six or thirteen days, test materials or an equivalent solvent were added into the medium and cultured for 24 hours before harvesting cells for RNA extraction.

For the *Ahr* gene knockdown, commercially synthesized siRNA against human *AhR* (s1200, Thermo Fisher, Waltham, MT, USA) was transfected by using a Silencer™ siRNA Transfection II Kit (Thermo Fisher) according to the manufacturer's instructions.

RNA was extracted using an RNeasy Mini Kit (Qiagen, Germany). A SuperScript™ VILO™ cDNA Synthesis Kit and an SYBR Green PCR Master Mix (Thermo Fisher) were used for cDNA synthesis and q-PCR. q-PCR was performed using StepOne Plus™ (Applied Biosystems, Foster city, CA, USA) and the results were analyzed by its software.

**Human test design to evaluate the postbiotic ingredient**

Thirteen healthy Japanese females and males aged 24 to 47 (average: 33.8 ± 5.8) participated in a single-blind study. A serum formula containing either 0%, 0.02%, or 1% postbiotic was applied twice daily to designated areas of the upper arm for one month. During the same period, a formula containing the postbiotic was applied twice daily to one side of the face, while a placebo formula was applied to the opposite side of the face. One male participant who exhibited an exceptionally high melanin index in the face was excluded from the statistical analysis of half-face test. Prior to the study, the minimal erythemal dose (MED) was determined for each volunteer on the arm opposite to the one used for the test. After one month of application, the upper arm area was exposed to UVB at 1.2 MED. For UV irradiation, Model 601 Multiport® SPF Testing 6 Output Solar simulator (Solar Light Co., Inc. Glenside, PA, USA) was used. 24 hours after exposure, a* was measured by CM-2600d (Konica Minolta, Tokyo, Japan). For both the half-face test and the arm test, changes in values following one month of application or after UVR exposure were calculated as percentages relative to the baseline. The test was approved by the Human Test Ethics Council of Shiseido Co., Ltd. under the approval number B10442.

## 3. Results

### Modulation of facial skin microbiome observed in the six months with the highest UVR

We investigated the cumulative influence of prolonged exposure to solar ultraviolet radiation (UVR) in daily life, with and without the use of SPF 50+ sunscreen on the facial skin microbiome. A total of 44 healthy Japanese women participated in the study. Among them, 22 were non-intensive sunscreen users (the “control group”), and 22 consistently used sunscreen with SPF 50+ (the “SPF 50+ group”). The ages of participants ranged from 40 to 55 with group averages of 47.4 ± 5.1 and 47.8 ± 4.4, respectively.

Instrumental skin measurement and stratum corneum sampling were conducted in Tokyo, Japan in March and September 2022. Japan experiences distinct seasons with UVR levels becoming highest during the summer months (June through August) and lowest during the winter months (December through February). March is the month with the lowest total UVR exposure over the previous six months, while September is the month with the highest total UVR exposure over the same period (7). By comparing the facial skin microbiome of subjects in two distinct groups in March and September, the effect of daily UVR exposure on the skin microbiome was expected to be elucidated.

As shown in **Fig. 1**, the shift in the average composition of skin microbiome genera from March to September is more apparent in the control group than in the SPF 50+ group.

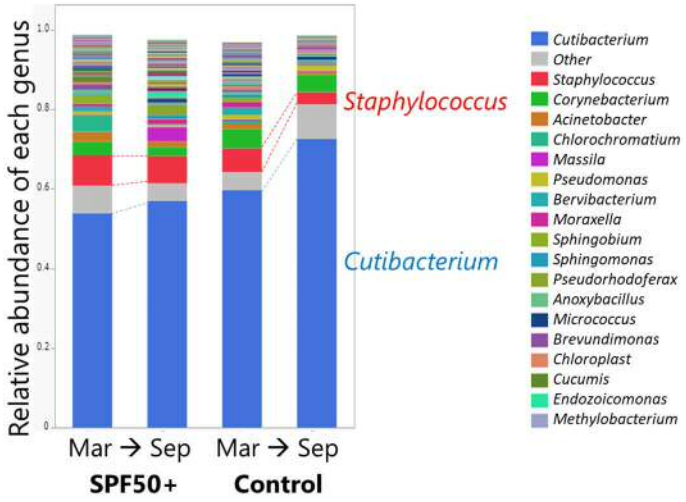


**Figure 1. Relative abundance of bacterial genera observed in the facial skin microbiome of the SPF 50+ group and control group in March and September (n = 22 each).**

In the control group, α diversity was significantly lower in September than March, regardless of indicators used, represented by the Shannon index in **Fig. 2a**. This decrease in α diversity was associated with the significant decrease in β diversity ($p$=0.0107, data not shown), indicating that the facial skin microbiomes of participants in the control group were more similar to one another in September than in March. Features of the skin microbiome shared among the control group in September were characterized by a higher relative abundance of *Cutibacterium* (**Fig. 2b**), while that of *Staphylococcus* was lower than in March (**Fig. 2c**).

In contrast, the facial skin microbiome of the SPF 50+ group did not show any significant differences between March and September. Neither α nor β diversity decreased during the six months (**Fig. 2e**). The relative abundance of *Cutibacterium* and *Staphylococcus* remained the same (**Fig. 2f** and **2g**). Only the absolute abundance of bacteria, which was estimated by the q-PCR results of 16S rRNA coding DNA, appeared significantly higher in September than March in the SPF 50+ group (**Fig. 2h**), while the increase was not significant in the control group (**Fig. 2d**). Even among the participants in the control group, the degree of change in

melanin levels from March to September varied among individuals, and the increase in absolute abundance of bacteria correlated negatively with the increase in melanin index (data not shown), suggesting the possibility that even without SPF 50+, less exposure to UV allows for an increase in bacteria from March to September.

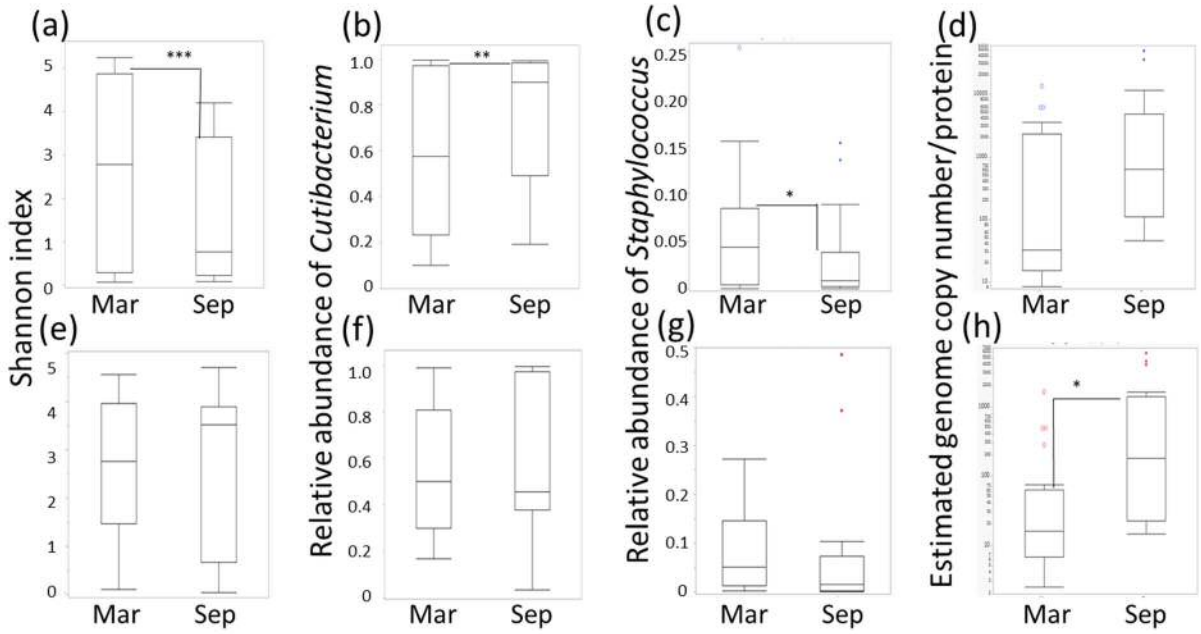


**Figure 2. Box plot presentation of the shift of skin microbiome parameters in the control (a-d) and SPF 50+ groups (e-h) from March to September:**
**(a, e)** The Shannon index only decreased significantly in the control group ($p$ = 0.0007) but did not change in the SPF 50+ group ($p$ = 0.7662). **(b, f)** Relative abundance of *Cutibacterium* increased significantly in the control group ($p$ = 0.0069), while it did not change in the SPF 50+ group ($p$ = 0.5775) **(c, g)**. Relative abundance of *Staphylococcus* decreased significantly in the control group ($p$ = 0.0397), while it did not change in the SPF 50+ group ($p$ = 0.7865). **(d,h)** Bacterial absolute abundance was estimated as the genome copy number based on the qPCR results using 16S rRNA-coding DNA and was normalized by the protein amount in the stratum corneum samples. While the difference between March and September was not significant in the control group ($p$ = 0.1002), a significant increase was observed in the SPF 50+ group ($p$ = 0.018). All statistical analyses were performed by a paired t-test, *** indicates $p$-value below 0.001, ** 0.001 < p < 0.01 and *0.01 < $p$ < 0.05.

## Development of a postbiotic to compensate for the weakening skin microbiome function

Based on these results, we aimed to develop a fermentation product (postbiotic) as an active ingredient specifically designed to compensate for skin microbiome functions that weaken due to UVR exposure. We focused particularly on their contribution to the skin's antioxidative and barrier functions.

For the antioxidative function of the skin microbiome, we identified a novel aspect of its contribution, in which ferulic acid (FA) is bioconverted to 4-vinylguaiacol (4-VG) by specific bacterial genera residing on the skin. The stratum corneum samples, collected using sterilized adhesive tape, were incubated in a medium containing ferulic acid, and 4-VG generation was observed in the culture in a ferulic-acid dependent manner (data not shown).

Subsequently, we isolated independent colonies from the stratum corneum samples using culture methods with various media and tested the 4-VG production capability of each strain. A small number of strains producing 4-VG from FA were discovered (**Fig. 3**). Those strains were identified as *Bacillus* sp. by sequencing 16S rRNA-coding DNA.

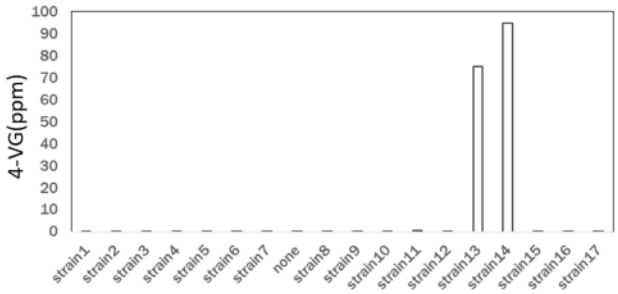


**Figure 3. 4-VG was detected in the bacteria culture of the strains isolated from stratum corneum grown in media supplemented with 100 ppm ferulic acid**.

4-VG by itself is known to exhibit higher antioxidative activity than FA (8). We further tested the effect of 4-VG in inducing the antioxidative capability in keratinocytes in comparison with FA. The expression of the *Nqo1*, *Sod3*, and *Hmox1* genes, which were located downstream of Nrf2, as well as that of *Cyp1A1* downstream of AhR, was upregulated by 4VG or FA supplemented at 1,10, or 100 uM, and it was found that 4-VG is more efficient in those activities than FA when compared to an equal molar concentration (**Fig. 4a**). We also confirmed that the effect of 4VG is exerted via AhR using siRNA targeting the *Ahr* gene (**Fig. 4b**).

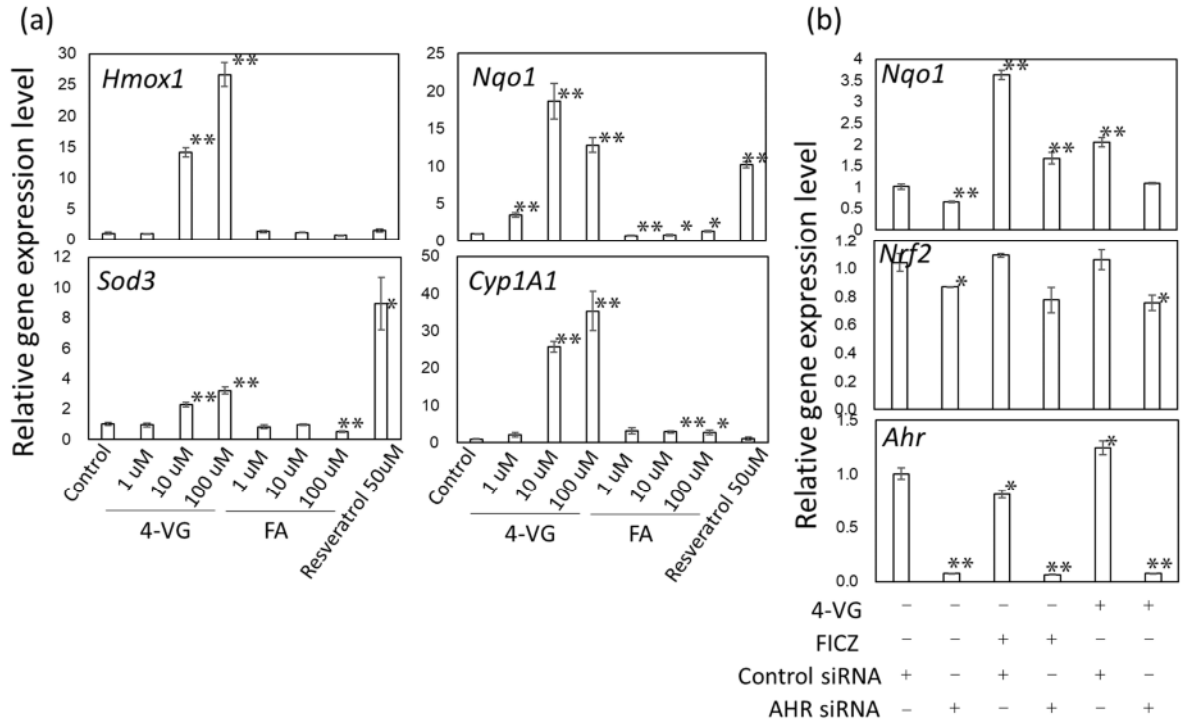


**Figure 4. Effect of 4-VG and FA on mRNA accumulation of anti-oxidative function-related genes (a)** 4-vinylguaiacol induces the expression of *Hmox1*, *Sod3*, *Nqo1*, and *Cyp1A1* more effectively than ferulic acid; **(b)** transfection of siRNA targeting the *Ahr* gene successfully resulted in the suppression of the *Ahr* gene expression and diminished the effect of FICZ or 4-VG to promote

the expression of *Nqo1* or *Nrf2*. Error bars indicate standard deviations. Statistical analyses were done by Student's t-test. n=3. *$p$<0.05, **$p$<0.01

In the development of a postbiotic ingredient, we chose to ferment a substrate rich in ferulic acid using yeast to include 4-VG as an active component. The resulting yeast ferment product was confirmed to have high efficacy in inducing those genes for an antioxidative function, i.e., *Nrf2*, *Nqo1*, and *Hmox1* (**Fig. 5a**). Furthermore, the same postbiotic shows upregulation of the *Flg*, *Lor*, and *Inv* genes (**Fig. 5b**), suggesting that this postbiotic could complement the barrier promoting function as well as the antioxidative function of the skin microbiome, such as *S.epidermidis*, which was found susceptible to UVR (**Fig. 1** and **Fig. 2c**). The expression of *Cyp1A1*, under the same AhR pathway as the genes in **Fig. 5a** and **5b**, was less or not upregulated by the postbiotic (**Fig. 5c**).

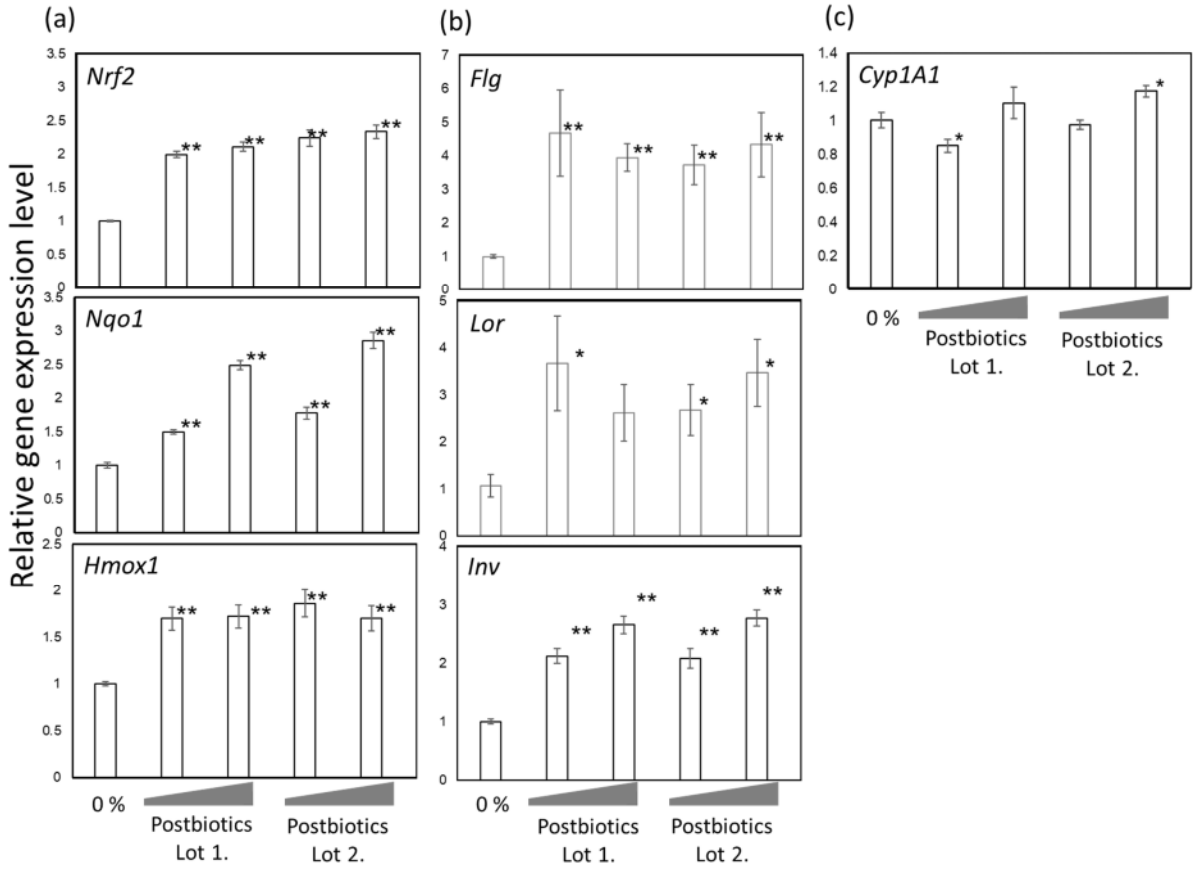


**Figure 5. Effect of the postbiotic on the mRNA accumulation of (a) antioxidative-function-related genes, i.e., *Nrf2*, *Nqo1*, and *Hmox1*; (b) cornified envelope-related genes, i.e., *Flg*, *Lor*, and *Inv*; and (c) xenobiotic degradation-related gene, i.e., *Cyp1A1*.** Error bars indicate standard deviations. Statistical analyses were done by Student's t-test. n=3. *$p$<0.05, **$p$<0.01.

The effectiveness of the postbiotic was further evaluated *in vivo* by a half-face test. The participants were asked to apply a formula containing the postbiotic to one side of their faces and a placebo on the other side for one month. Due to seasonal changes during the test period from March to April, facial skin tended to accumulate more melanin after one month of application than before. However, we observed that this increase in melanin index was significantly

smaller on the side treated with the formula containing the postbiotic than the placebo side (**Fig. 6a**) ($p$ = 0.032, paired t-test). Concomitantly, the degree of increase in b* during the test period was also smaller on the postbiotic-treated side than the placebo side (**Fig. 6b**), although the difference was not statistically significant ($p$ = 0.1887, paired t-test). These results support the positive effect of our postbiotic in preventing an oxidative reaction caused by daily UVR exposure.

Furthermore the postbiotic's *in vivo* efficacy in mitigating erythema caused by UVR exposure was confirmed via a controlled arm test conducted in parallel with the half-face test, where participants applied the postbiotic or placebo to small designated regions on their upper arms. After one month of application, skin color parameters were measured in the test region and then UVR (UVB + UVA) was exposed at 1.2 MED as previously determined. Skin color was measured in the same manner 24 hours after exposure. The a* values (indicative of erythema caused by UVR exposure) exhibited increases in both the postbiotic- and placebo-treated regions, but the increase was significantly smaller in the postbiotic-treated region (**Fig. 6c**).

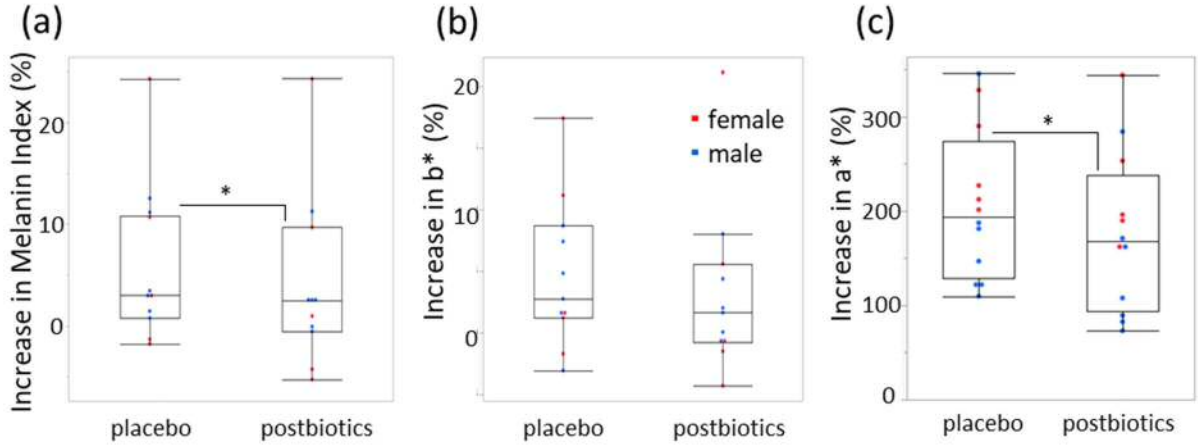


**Figure 6. *In vivo* effects of the postbiotic evaluated in the human test using (a, b) half-face and (c) upper arm** **(a)** Box plots showing that, during the one-month application period, melanin levels increased on both sides of the face, but the increase was significantly smaller on the side treated with the postbiotic than the equivalent formula without the postbiotic (placebo) ($p$ = 0.0107, paired t-test). **(b)** Box plots showing that the increase in b* value was also smaller on the postbiotic-treated side than the side treated with the placebo in the same human test ($p$ = 0.1887, paired t-test). **(c)** Box plots showing that the increase in a* value, measured 24 hours after UVR exposure, in small regions of the uppoer arms treated with the postbiotic or placebo for one month was found to be significantly smaller in the area treated with the postbiotic than the placebo ($p$ = 0.0225, paired t-test).

## 4. Discussion

The harsh conditions of the skin's environment—characterized by dryness, salinity, and acidity—limit the diversity of microbial species, predominantly favoring *Cutibacterium* and *Staphylococcus* (9). These microorganisms are integral to the skin's defense mechanisms, yet their balance can be disrupted by various factors, including UVR exposure. The present study clearly demonstrated that UVR in daily life significantly modulates the composition of the skin microbiome, especially the balance between *Cutibacterium* and *Staphylococcus*, and this disruption can be mitigated with sufficient sunscreen application (**Fig. 1** and **Fig. 2**).

Furthermore, UVR exposure exerts a stronger influence on the skin microbiome than other seasonal factors such as increased sweat and sebum production associated with higher temperatures. Immunosuppression induced by UVR may also lead to an increase in bacterial abundance as skin immunity suppresses the skin microbiome. However, the SPF 50+ group experienced a greater increase than the control group (**Fig. 2d** and **2h**)., indicating UVR-induced immunosuppression may contribute less than UV's bactericidal effect or other factors such as sebum and sweat in the control of the skin microbiome. Interestingly, the sebum secretion rate increased significantly in September compared to March only in the control group (data not shown), yet this did not correspond with an increase in absolute bacterial abundance in the control group. This suggests that the negative effects of UVR may outweigh the positive effect of higher sebum secretion.

UVR exposure induces oxidative stress in the skin via formation of reactive oxygen species (ROS), and members of the skin microbiome, such as *S.epidermidis*, are known to protect the skin from this stress by secreting antioxidative enzymes such as superoxide dismutase (10). In addition, *S.epidermidis* promotes skin barrier formation by inducing the expression of related genes in keratinocytes (11). It was revealed that another genus in the skin microbiome, *Bacillus sp.* bioconverts plant-origin phenolic antioxidant ferulic acid (FA) to yield a more potent antioxidant, 4-vinylguaiacol (4-VG) (**Fig. 3** and **Fig. 4**). The gene responsible for this activity in *Bacillus* has been reported previously (12). *Bacillus* has also been reported to suppress *Staphylococcus aureus*, a malignant member of the skin microbiome (13). Indeed we confirmed that the strains of *Bacillus* that we isolated clinically also inhibited *S.aureus* propagation (data not shown). Therefore, *Bacillus* seems to be a promising candidate as a probiotic for future skincare applications. Overall, the skin microbiome plays an important role in preventing oxidative stress and maintaining a healthy skin barrier. However, the *S.epidemidis* and *Bacillus* responsible for that role decrease in relative abundance during the six months of high UVR exposure. Harel *et al*., reported that enrichment of *Sphingomonas*, which reduces ROS generated by UVR exposure, was observed in the arm skin microbiome of ten lifeguards during summer by comparing October to May (13) but such shift was not observed in the present study probably due to the difference in the body sites used in the tests and/or the life environment of participants.

Therefore, we aimed to develop a postbiotic to compensate the loss of function, hoping to alleviate damage in skin caused by UVR exposure. *In vitro* studies confirmed the expected efficacy of the antioxidative and barrier functions (**Fig. 5**). In the human study, we found that the basic formula supplemented with this postbiotic suppressed increases in melanin and b* in facial skin (**Fig. 6a** and **6b**), which is likely due to the suppression of oxidative stress caused by UVR directly through blocking UV or erasing ROS by molecules in the postbiotics, including ferulic acid and 4VG. Also, enhancement of the anti-oxidative gene expression by those molecules strengthens the skin's resilience to oxidative stress. We also confirmed that the degree of erythma caused by artificial UVB exposure to the upper arm was lessened in the region which had been treated with the formula containing the postbiotic (**Fig. 6c**).

## 5. Conclusion

In this study, we present a comprehensive approach toward the development of future UV care products, beginning with fundamental research and culminating in the development of an active ingredient. We investigated how daily exposure to UVR modulates the skin microbiome in complex interaction with other factors. Significant modifications were observed, and it was clear that those changes were due to UVR, as application of high-SPF sunscreen reverted them. These findings conclude the necessity for an active ingredient to compensate the lost functions of the skin microbiome after UVR exposure in order to mitigate skin damage. To

address this need, we focused on postbiotics and designed a targeted fermentation process to achieve desired efficacy proven *in vitro* and *in vivo*. By formulating sunscreen and other suncare products with these postbiotics, we will deliver new value for skincare inspired by the skin microbiome function.

## References

**1.** Gilchrest BA (1995) Dermatoheliosis (Sun-induced aging). in: Gilchrest BA, ed.: Photodamage. Cambridge USA, Blackwell Science Inc. pp 97-116.
**2.** Burns EM, Ahmed H, Isedeh PN, Kohli I, Van Der Pol W, Shaheen A, Muzaffar AF, Al-Sadek C, Foy TM, Abdelgawwad MS, Huda S, Lim HW, Hamzavi I, Bae S, Morrow CD, Elmets CA, Yusuf N. Ultraviolet radiation, both UVA and UVB, influences the composition of the skin microbiome. Exp Dermatol. 2019 Feb;28(2):136-141. doi: 10.1111/exd.13854. Epub 2019 Jan 14. PMID: 30506967; PMCID: PMC7394481.
**3.** Schuetz R, Claypool J, Sfriso R, Vollhardt JH. Sunscreens can preserve human skin microbiome upon erythemal UV exposure. Int J Cosmet Sci. 2024 Feb;46(1):71-84. doi: 10.1111/ics.12910. Epub 2023 Oct 6. PMID: 37664974.
**4.** Patra V, Byrne SN, Wolf P. The Skin Microbiome: Is It Affected by UV-induced Immune Suppression? Front Microbiol. 2016 Aug 10;7:1235. doi: 10.3389/fmicb.2016.01235. PMID: 27559331; PMCID: PMC4979252.
**5.** Callahan, B.J., McMurdie, P.J., Rosen, M.J., Han, A.W., Johnson, A.J., Holmes, S.P. (2016). DADA2: High resolution sample inference from Illumina amplicon data. Nat Methods 13(7):581-3. doi: 10.1038/nmeth.3869
**6.** Caporaso, J.G., ... Knight R. (2010). QIIME allows analysis of high-throughput community sequencing data. Nat Methods (7): 335-336. doi: 10.1038/nmeth.f.303
**7.** https://www.data.jma.go.jp/env/uvindex/en
**8.** Azadfar M, Gao AH, Bule MV, Chen S. Structural characterization of lignin: a potential source of antioxidants guaiacol and 4-vinylguaiacol. Int J Biol Macromol. 2015 Apr;75:58-66. doi: 10.1016/j.ijbiomac.2014.12.049. Epub 2015 Jan 17. PMID: 25603142.
**9.** Byrd AL, Belkaid Y, Segre JA. The human skin microbiome. Nat Rev Microbiol. 2018 Mar;16(3):143-155. doi: 10.1038/nrmicro.2017.157. Epub 2018 Jan 15. PMID: 29332945.
**10.** Kaneko A, Kondo S, Akiyama J, Okabe K. Delivery method of SOD to the skin by using Mn/Zn-containing lotion which promotes SOD secretion in Staphylococcus epidermidis, Drug Delivery System, 1997, 12(5): 339-345 doi.org/10.2745/dds.12.339
**11.** Landemaine L, Da Costa G, Fissier E, Francis C, Morand S, Verbeke J, Michel ML, Briandet R, Sokol H, Gueniche A, Bernard D, Chatel JM, Aguilar L, Langella P, Clavaud C, Richard ML. *Staphylococcus epidermidis* isolates from atopic or healthy skin have opposite effect on skin cells: potential implication of the AHR pathway modulation. Front Immunol. 2023 May 26;14:1098160. doi: 10.3389/fimmu.2023.1098160. PMID: 37304256; PMCID: PMC10250813.
**12.** Degrassi G, Polverino De Laureto P, Bruschi CV. Purification and characterization of ferulate and p-coumarate decarboxylase from Bacillus pumilus. Appl Environ Microbiol. 1995 Jan;61(1):326-32. doi: 10.1128/aem.61.1.326-332.1995. PMID: 7887611; PMCID: PMC167286.
**13.** Piewngam P, Zheng Y, Nguyen TH, Dickey SW, Joo HS, Villaruz AE, Glose KA, Fisher EL, Hunt RL, Li B, Chiou J, Pharkjaksu S, Khongthong S, Cheung GYC, Kiratisin P, Otto M. Pathogen elimination by probiotic Bacillus via signaling interference. Nature. 2018 Oct;562(7728):532-537. doi: 10.1038/s41586-018-0616-y. Epub 2018 Oct 10. PMID: 30305736; PMCID: PMC6202238.
**14.** Harel N, Ogen-Shtern N, Reshef L, Biran D, Ron EZ, Gophna U. Skin microbiome bacteria enriched following long sun exposure can reduce oxidative damage. Res Microbiol. 2023 Nov-Dec;174(8):104138. doi: 10.1016/j.resmic.2023.104138. Epub 2023 Sep 16. PMID: 37722498.